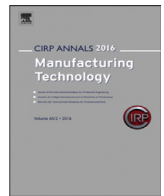




Contents lists available at ScienceDirect

CIRP Annals - Manufacturing Technology

journal homepage: <https://www.editorialmanager.com/CIRP/default.aspx>

Creasing and folding of paper-based sandwich material—Phenomena and modelling

E. Simonetto^a, P. Singh^a, A. Ghiotti (1)^{a,*}, S. Bruschi (1)^a, N. Jessen^b, P. Groche (1)^b^a Department of Industrial Engineering (DII), University of Padova, Padova, Italy^b Institute for Production Engineering and Forming Machines, Technische Universität Darmstadt, Darmstadt, Germany

ARTICLE INFO

Article history:
Available online xxx

Keywords:
Forming
Delamination
Packaging

ABSTRACT

Creasing and folding are fundamental steps in many manufacturing processes of multi-material paperboard packaging. The complex structure of these materials, which comprise layers of cellulose fibres, aluminium, and polyethylene, coupled with the growing complexity of packaging designs, make these process operations essential to ensure the required structural integrity for packaging as well as their functionality in daily life. This paper introduces an approach for modelling damage in paper-based sandwich materials by integrating fibre-based and cohesive numerical modelling techniques. The results prove the effectiveness of the proposed methodology, opening new possibilities for process design and optimization in packaging manufacturing.

© 2024 The Author(s). Published by Elsevier Ltd on behalf of CIRP. This is an open access article under the CC BY-NC-ND license (<http://creativecommons.org/licenses/by-nc-nd/4.0/>)

1. Introduction

The evolution of packaging technology within the food and beverage sectors has emphasized the need for a deeper knowledge of paperboard materials as well as accurate modelling of their behaviour in many packaging shaping operations, such as creasing and folding [1]. Their wide variety and complex nature further complicate the achievement of reliable and optimized processes that are essential to attain the desired functionality and maintain the necessary structural integrity. In addition to the mechanical requirements, paperboard must also fulfil a range of criteria across chemical, optical, aesthetic, and economic domains, requiring a level of versatility unattainable with a single material [2]. This complexity is compounded in multi-material paperboard, where various plies and additional layers, such as aluminium foil or polyethylene, are amalgamated with cellulose fibres, thus making the response of the sandwich structure even more complex [3]. Consequently, incorrect setting of creasing parameters can result in a loss of folding accuracy or lead to localized defects, posing contamination risks.

The empirical understanding of creasing and folding processes has historically driven the development of continuum mechanics models, based on traditional mechanical properties such as yield and strength values [4], anisotropy behaviour [5] and formability [6]. The transition to more advanced material models, such as those represented by discrete material models is ongoing, particularly in understanding the damage behaviour.

Continuum mechanics models have faced challenges particularly in accurately capturing the local inhomogeneities that arise during localized paperboard deformation and in reliably predicting the

anisotropic behaviour of damage evolution in these materials [7]. Despite advancements in material science and computational capabilities, continuum models still struggle to effectively represent the interactions between various material layers, especially under the complex loading conditions of creasing and folding [8]. Creasing introduces localized damage to facilitate subsequent folding, predominantly through shear deformations causing material delamination. Current continuum models often fail to capture the onset and progression of this damage accurately, resulting in a gap between the predicted and actual material behaviour during and after the creasing process.

Among discrete modelling techniques, fibre-based models have demonstrated their reliability in providing an accurate representation of the fibre structure of paperboard. These models focus on individual fibres' behaviour within the material matrix, offering insights into the micro-level mechanical interactions. However, they also face significant challenges in scaling up to predict the behaviour of the multi-material paperboard structure with complex deformations [9]. Further limitations of the fibre-based models affect the damage propagation or plies separation when material fibres are modelled [10]. Another challenge for both continuum and fibre-based models is the representation of the anisotropic behaviour of paperboard. The significant differences in stiffness and yield stress in the machine, cross and thickness directions make it difficult for these models to accurately capture the mechanical response of paperboard under creasing and folding stresses. This challenge is compounded by the need to model the complex interplay of in-plane and out-of-plane behaviours, along with the potential for delamination and other damage mechanisms [2,11]. In conclusion, while significant progress has been made in developing models for the mechanical behaviour of paperboard in packaging applications, substantial challenges remain. The accurate prediction of fibre damage in multi-material paperboard

* Corresponding author.

E-mail address: andrea.ghiotti@unipd.it (A. Ghiotti).

<https://doi.org/10.1016/j.cirp.2024.04.027>

0007-8506/© 2024 The Author(s). Published by Elsevier Ltd on behalf of CIRP. This is an open access article under the CC BY-NC-ND license (<http://creativecommons.org/licenses/by-nc-nd/4.0/>)

is not yet widely explored and local fibre behaviour, when scaled to the process size, remains unaddressed.

The paper presents a novel approach to integrate fibre-based modelling and inter-ply damage propagation in multi-material paperboard creasing and folding. Unlike the approaches available in the state-of-the-art, the main innovations introduced are (i) the integration of continuum and fibre-based modelling to accurately represent the material behaviour of the various plies, and (ii) the full coupling of intra-ply damage and inter-play delamination within chained FE simulations of creasing and folding operations. After the description of an industrial case taken as reference, the experimental characterization of the paperboard material and the mechanical properties are outlined. Then, modelling of the bonding strength, developed based on the cohesive zone theory, is presented. Finally, the proposed method is validated on a laboratory-scale industrial case.

2. Process chain

Gable top packaging for beverages has been taken as a reference case due to the number and complexity of creasing and folding operations implemented in the process chain. Fig. 1(a) illustrates a typical gable top container for liquids, produced through a series of folding operations along creasing lines, preliminary realized on flat multi-material paperboard. Fig. 1(b) shows the intricate pattern of creasing lines, which exhibit various orientations relative to the calendering direction. The creasing operation involves applying mechanical pressure via a creasing rule or die onto the paperboard surface, as depicted in Fig. 1(c). As a result, localized deformation is induced on the paperboard fibres, which reduces the material's resistance to bending, allowing for smooth and precise folds along the crease line. Subsequently, folding is carried out along the creased groove, on both the concave, Fig. 1(c), and convex, Fig. 1(e), sides, resulting in different positioning of the Al barrier and, consequently, loading conditions. This complexity necessitates careful selection of process parameters, particularly at corners where multiple grooves converge.

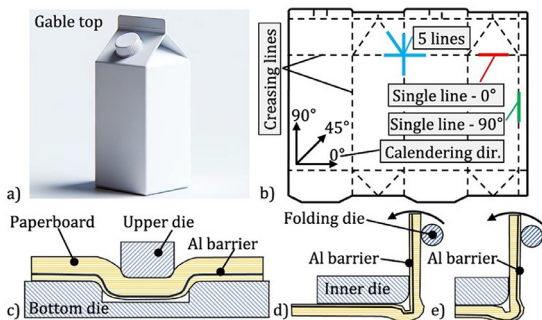


Fig. 1. (a) Gable-top packaging, (b) creasing lines on the calendered paperboard, (c) creasing operation, (d) inner and (e) outer folding.

3. Experimental

The study case material is a five-layer multi-material paperboard, commonly used in gable-top containers for liquids. This paperboard consists of a three-ply cellulose fibre board sandwiched between layers of polyethylene (PE) and aluminium (Al) foil, both coated externally with PE. The three-ply cellulose fibre construction consists of a top and bottom ply made of bleached sulphate pulp and a mid-ply made of chemi-thermomechanical pulp. Fig. 2(a) and (b) respectively show the schematic representation of the layers' disposition in the cross-section, including the average thickness of each ply and the paperboard cross-section measured by an X-ray Computed Tomography (CT) Nikon Metrology MCT225. CT measurements allowed evaluating the fibres' orientation, density, and length in each ply, see Fig. 2 (c) and (d), showing that the fibres fraction is lower in the mid-ply compared to the outer plies, see Fig. 2(e). The fibres' length is reported in Table 1.

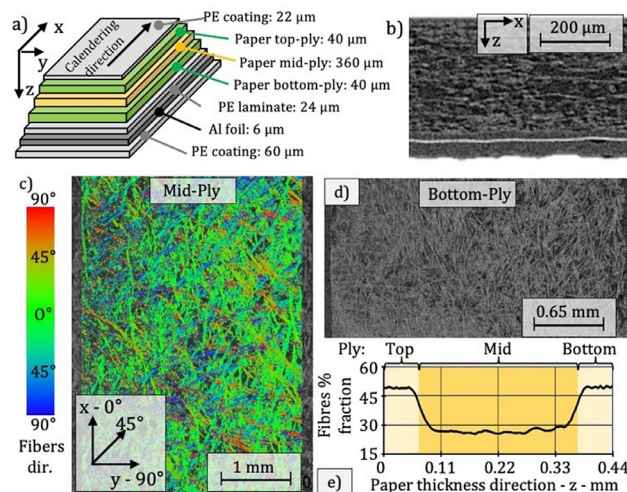


Fig. 2. (a) Schematic representation of the paperboard cross-section, (b) CT scan of the paperboard cross-section, (c) top view CT of the middle and (d) outer ply, and (e) fibres fraction in the cross-section.

Table 1
Fibre's length in paperboard plies.

Paper Ply	Top	Middle	Bottom
Fibres length	1.44±0.44 mm	1.18±0.42 mm	1.51±0.49 mm

The mechanical properties were investigated using a 15 kN MTS™ 858 Mini Bionix II servo-hydraulic dynamometer. Mechanical testing was conducted not only on the five-layer paperboard but also on three-ply cellulose structures, both with and without PE layers and coatings. Fig. 3 shows the results of the tensile tests carried out in three different directions, respectively 0, 45 and 90 deg, relative to the calendering direction. They demonstrate that the anisotropic behaviour of the paperboard is predominantly due to the alignment of cellulose fibres during the calendering process, as illustrated in Fig. 2(c). The increase of the flow stress values can be primarily attributed to the PE layers, whereas the Al foil appears to contribute minimally to the strength of the paperboard, regardless of the tested directions.

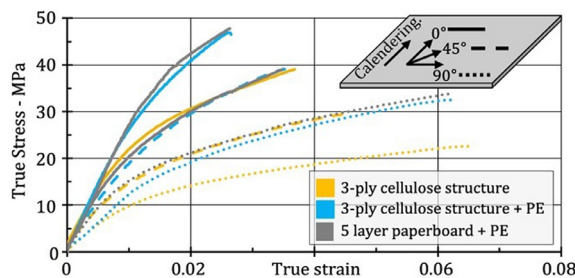


Fig. 3. Eng. stress-strain curves at varying calendaring directions.

To test the adhesion strength of the joints, both lap-shear and normal-separation tests were conducted with repeatability 5 following the EN 1465 and EN ISO 11339 standards (See Fig. 5).

4. Modelling

4.1. Paperboard modelling

The paperboard material was modelled integrating continuum mechanics and fibre-based approaches. Specifically, the power law material model was applied to the PE ($K = 55 \text{ MPa}$, $n = 0.32$ [12]) and Al ($K = 110 \text{ MPa}$, $n = 0,03$ [13]) and these layers were modelled with fully integrated isotropic solid elements. The in-plane behaviour of the three-ply cellulose structure was represented through a

stochastic network of beam elements, with their out-of-plane behaviour constrained within solid elements. Fig. 4(a) presents the algorithm developed for the stochastic generation of the beam network within each layer. In the first step, it calculates the force that a ply cross section can withstand in each direction, based on the assumption that fibres response is solely axial, given their low bending stiffness. This is expressed by the Eq. (1):

$$F_{\theta} = \sum_{i=1}^N AK(\varepsilon_{\theta_i} \cos(\theta_i))^n \cos(\theta_i) \quad (1)$$

where θ represents the direction relative to the paperboard calendaring process, N denotes the number of fibres interesting the section, A is the equivalent beam cross section, K and n are the power law constants. As the fibres are distributed along the, 0° , 45° , and 90° directions, then Eq. (1) can be computed as shown in Fig. 4a. To ensure that the total volume of distributed fibres, remains constant across the different layers, the following relationship is maintained, Eq. (2):

$$\frac{N_0 + N_{45} + N_{90}}{N} = 1. \quad (2)$$

The percentage of fibres in each ply were then computed by numerical fitting the experimental results from tensile tests carried out in each direction. This approach demonstrated its effectiveness, as proved by the alignment of the computed values with the results of the CT measurements showed in Fig. 4(b). The maximum deviation of 8.6 % and 2.1 % were observed respectively for N_0 and N_{90} , while a lower deviation was obtained for N_{45} .

In the second step, beam elements were generated by meshing the modelled volume into sub-units. To achieve a homogeneous distribution of fibres within each sub-unit, the starting point of each fibre is randomly generated, while the endpoint is established according to the fibre's preferential orientation. The number of beams created for each direction corresponds to the fibre percentage distribution previously calculated. These beams were modelled to have an average length L , with the standard deviation as measured by the CT scans (see details in Table 1). Fig. 4(c) illustrates an example of a generated fibre network, while Fig. 4(d) shows the developed FE model, showcasing both the fibres and the distribution of the elements within each ply. To account for variations in fibre density and length, distinct beam networks were created for each paper ply. The flow stress behaviour of these fibres was modelled using the power law fitting of the experimental results, with $K = 6240$ MPa and $n = 0.66$. Since the beam elements, submerged within the solid ones, could move independently, a coupling was introduced to constrain their nodes velocity to be the same [14]. Considering the varying thickness of the layers, all were modelled with a single element in thickness, except for the paper mid-ply which was modelled with seven elements to maintain a consistent elements size across the plies.

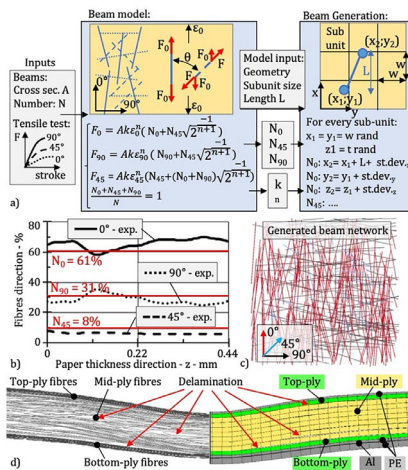


Fig. 4. (a) Algorithm for the beam generation, (b) percentage of fibres in the different directions, (c) example of generated beams, and (d) numerical FE model of the creasing operation.

4.2. Laminate structure modelling

The multilayer nature of the paperboard means that especially out-of-plane loads may lead to delamination, either between the different layers or within the mid-ply itself. To model the interface conditions between the different layers, a bilinear traction-separation model dependent on the fracture mode (either normal (Mode I), tangential (Mode II), or mixed) was implemented [15]. Fig. 5 shows the implemented models, based on the results of the normal and lap-shear separations tests introduced in paragraph 3.2. The stress (σ) and strokes (δ) for mode I and mode II, have been normalized with respect to the maximum values reached by the mid-ply internal interface, with a peak stress σ_I and σ_{II} respectively of 0.23 and 1.36 MPa, and maximum strokes δ_I and δ_{II} of 0.41 and 0.49 mm. Taking as reference the energy release rate E to evaluate the overall interface strength, for mode I, E_I between the paper outer and middle plies is 2.5 % higher with respect to the mid-ply inner interface, while for mode II, E_{II} is 162 % higher. Considering the Al-PE interfaces the E_I and E_{II} increments are respectively of 88 % and 262 %, while for the PE-paper interfaces the increments are of 43 % and 49 %. Therefore, the experimental results demonstrate that the mid-ply is the most susceptible to delamination, primarily due to its lower fibre density as highlighted by Fig. 2(c) and (e).

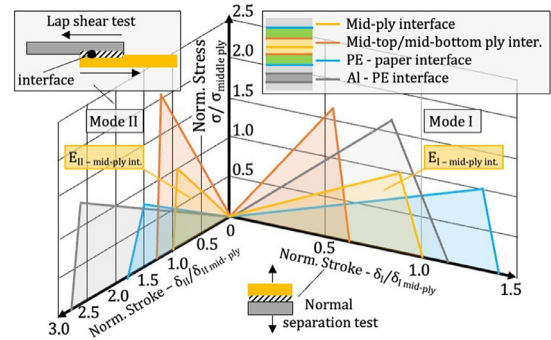


Fig. 5. Traction-separation model.

5. Validation

The methodology employed was substantiated through creasing and folding operations, executed within a controlled laboratory setting. The paperboard underwent stamping utilizing a 50 kN MTS™ dynamometer, operating at a speed of 20.0 ± 0.1 mm/s. To closely monitor the forming loads in the folding operation, an additional ± 10.0 N load cell was integrated in the dies. Efforts were made to closely emulate industrial conditions during these tests, which included maintaining ambient room temperature and monitoring average humidity levels, consistently observed to be approximately 55 %. Fig. 6 illustrates the modular equipment engineered for executing both creasing and folding operations. The apparatus comprises a die-set, Fig. 6(a), which accommodates modular dies to carry out different creasing configurations, see Fig. 6(c), as well as the final folding, Fig. 6(b). Fig. 7(a) shows the CT cross-sections of a creased

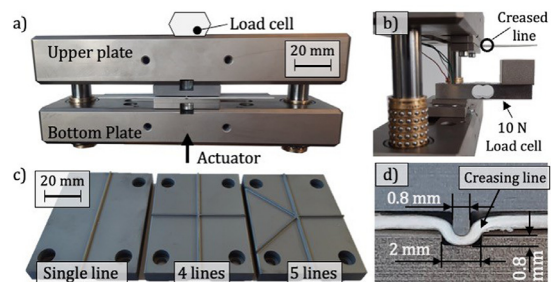


Fig. 6. (a) Experimental set-up for the creasing and (b) folding tests. (c) Detail of the crease lines and (d) dimensions of the creasing groove.

sample, the numerical model of which was depicted in Fig. 4(d). The numerical and experimental results verify that the creasing process causes localized delamination, especially in the lower-density mid-ply. This delamination is primarily found in areas with higher curvature gradients.

Fig. 7(b) compares the creasing forces at 0 and 90-degree orientations. The results indicate that the creasing force is greater when performed orthogonal to the calendaring direction, attributed to the increased number of stretched fibres. In this scenario, the FE model predicts the force trend with a maximum deviation of 17%. It also identifies a sharp force increment at a punch stroke of 1 mm, after which the paper reduces in thickness. Furthermore, the convergence of multiple creasing lines at the same point leads to more complex stress states in the area, thereby increasing the required force. This increase is evident in the results for the 4- and 5-way cases. In the creasing operation, the Al layer is always positioned on the paperboard bottom side. However, folding can be executed either internally or externally, see Fig. 1(c). The former scenario is depicted in Fig. 8 (left side), where it is shown that delamination primarily occurs in the mid-ply of the cellulose fibres. In contrast, the latter scenario, shown in Fig. 8 (right side), features delamination on both sides adjacent to the fold. Fig. 8(b) presents a diagram comparing experimental and numerical torque, indicating a maximum error of 11%. In this context, folds made orthogonal to the lamination direction require greater force. Similarly, outer folds demand more force than inner ones due to the higher load needed to deform the fibres compared to that required for ply delamination.

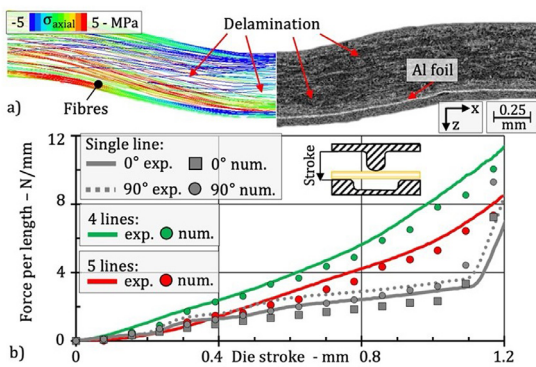


Fig. 7. (a) CT cross-section and (b) creasing forces.

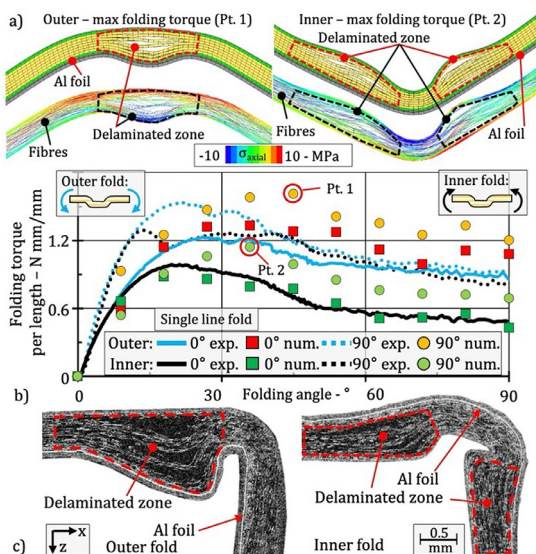


Fig. 8. Paperboard folding with outer (left) and inner creasing (right): (a) FE results, (b) folding torque diagram, and (c) CT scans.

6. Conclusions

The paper presents a methodology for simulating damage in multi-material paperboard during creasing and folding operations, combining fibre-based and cohesive numerical modelling techniques. The primary novelties of this approach include (i) calibrating the material properties of each paperboard ply, considering the distribution of fibre percentages; (ii) integrating continuum and fibre-based modelling to accurately represent the material behaviour of the various plies, and (iii) coupling the intra-ply damage and inter-ply delamination within FE simulations of creasing and folding operations. The numerical model has been validated by experimental tests, based on CT scans. The outcomes substantiate the model's proficiency in predicting fibre behaviour during deformation. This enables the estimation of failure and delamination, as well as the computation of forming loads, with a maximum deviation of about 17% and 11% from the values measured in experiments respectively for the creasing and folding operation.

Declaration of competing interest

The authors declare that they have no known competing financial interests or personal relationships that could have appeared to influence the work reported in this paper.

CRediT authorship contribution statement

E. Simonetto: Data curation, Formal analysis, Investigation, Software, Validation, Visualization, Writing – original draft, Writing – review & editing. **P. Singh:** Data curation, Formal analysis, Investigation, Resources, Validation. **A. Ghiotti:** Conceptualization, Funding acquisition, Investigation, Methodology, Project administration, Supervision, Validation, Writing – original draft. **S. Bruschi:** Conceptualization, Methodology, Supervision, Validation, Writing – original draft. **N. Jessen:** Data curation, Investigation, Writing – original draft, Writing – review & editing. **P. Groche:** Conceptualization, Supervision, Validation, Writing – original draft.

References

- [1] Simon JW (2021) A Review of Recent Trends and Challenges in Computational Modeling of Paper and Paperboard at Different Scales. *Archives of Computational Methods in Engineering* 28:2409–2428.
- [2] Barbier C, Larsson PL, Ostlund S (2006) On the Effect of High Anisotropy at Folding of Coated Papers. *Composite Structures*.
- [3] Huang H, Hagman A, Nygård M (2014) Quasi Static Analysis of Creasing and Folding for Three Paperboards. *Mechanics of Materials* 69(1):11–34.
- [4] Nagasawa S, Fukuzawa Y, Yamaguchi T, Tsukatani S, Katayama I (2003) Effect of Crease Depth and Crease Deviation on Folding Deformation Characteristics of Coated Paperboard. *Journal of Materials Processing Technology* 140(1-3):157–162.
- [5] Beex LAA, Peerlings RHJ (2009) An Experimental and Computational Study of Laminated Paperboard Creasing and Folding. *International Journal of Solids and Structures* 46(24):4192–4207.
- [6] Groche P, Huttel D (2016) Paperboard Forming - Specifics Compared to Sheet Metal Forming. *BioResources* 11(1):1855–1867.
- [7] Kulachenko A, Uesaka T (2021) Direct Simulations of Fiber Network Deformation and Failure. *Mechanics of Materials* 51:1–14.
- [8] Domaneschi M, Perego U, Borgqvist E, Borsari R (2017) An Industry-Oriented Strategy for the Finite Element Simulation of Paperboard Creasing and Folding. *Packaging Technology and Science* 30:269–294.
- [9] Nygård M, Sjökvist S, Marin G, Sundström J (2019) Simulation and Experimental Verification of a Drop Test and Compression Test of a Gable Top Package. *Packaging Technology and Science* 32:325–333.
- [10] Giampieri A, Perego U, Borsari R (2011) A Constitutive Model for the Mechanical Response of the Folding of Creased Paperboard. *International Journal of Solids and Structures* 48(16-17):2275–2287.
- [11] Nygård M (2009) Modelling the Out-of-Plane Behaviour of Paperboard. *Nordic Pulp & Paper Research Journal* 24(1):72–76.
- [12] Ghiotti A, Bruschi S, Simonetto E, Gennari C, Calliari I, Bariani P (2018) Electroplastic Effect on AA1050 Aluminium Alloy Formability. *CIRP Annals* 67(1):289–292.
- [13] Storsanso: NaturaTM Al93M Boar datasheet, 2018.
- [14] Hayashi S, Wu CT, Hu W, Wu Y, Pan X, Chen H (2019) New Methods for Compression Molding Simulation and Component Strength Validation for Long Carbon Fiber Reinforced Thermoplastics. *12th European LS-DYNA Conf., Koblenz, Germany*.
- [15] Guo Q, Yao W, Li W, Gupta N (2020) Constitutive Models for the Structural Analysis of Composite Materials for the Finite Element Analysis: A Review of Recent Practices. *Composite Structures* :113267.